# steel surface defect detection and localization based on SVD and two-side compressive measurements

Jingli Gao[1], Chenglin Wen*[2], Meiqin Liu[1]
1. College of Electrical Engineering, Zhejiang University, Hangzhou 310027, China
E-mail: gjl991@163.com;liumeiqin@zju.edu.cn
2. College of Electrical Engineering, Henan University of Technology, Zhengzhou 450001, China
E-mail: wencl@hdu.edu.cn

**Abstract:** This paper proposes a method for defect detection and localization based on singular value decomposition and two-side compressive measurements. First, the feasibility of the singular value decomposition for defect detection and localization is analyzed, then the invariance of the geometrical structure of the rows or columns of the raw data and the compressive data is justified, so the energy and pattern contained in the raw data can be transferred into the compressive data and kept in the singular values and singular vectors. On this basis, the proposed defect detection algorithm based on the singular values of compressive data and the proposed defect localization algorithm based on the singular vectors are given without reconstruction of images. Simulation results show that the proposed method based on compressive measurements has a good performance.

**Key Words:** defect detection, compressed sensing, singular value decomposition, random projection

## 1 INTRODUCTION

Cold rolled strip is the raw materials essential for automobile, shipbuilding, electrical appliance and other industries. The defects of strip surface directly affects the appearance quality, wear resistance and subsequent manufacturability, and is also the key indicators of market competition. Therefore, defect detection has become an important research topic in the field of computer vision[1]-[5].

Defect detection is to find the pixels whose values are deviated from the ones around them in an image[6]. When a defective product is to be tested, its imaging of the defect region has abnormal pixel values compared to the pixel values of the normal region. Usually in the process of imaging for products, due to the influence of light, surface smoothness and imaging equipment noise and other factors, the pixel values of images acquired at different time would be fluctuated within a certain range. If the shooting environment is kept the same, then the two normal images will be slightly different in the corresponding pixel values. However, if one of the two images is a defect image, the pixel values in the defective region have obvious difference with the normal pixel values. Accordingly, the differences in the gray values can be used to determine whether an image is defective.

The traditional detection methods often make use of various transformations for image compression, and then transmit the codes. When the receiver receives the transmitted information, reconstructs the image from the codes, and further detects flaw information from the reconstructed image. The typical methods include mathematical morphology and fractal based defect detection method[7]-[8], Gabor wavelet and variance based on thin steel defect detection algorithm[9], the Hough transform and principal component analysis based defect detection algorithm for welds, imprinting and holes[10], max-pooling convolution neural networks based defect detection method[11], the lower envelope and Weber contrast based pit defects detection[12], to name a few.

The above methods are carried out on the whole images through compression, reconstruction and further testing. Because of the drawbacks of Nyquist sampling for oversampling first and then compressing, compressed sensing has been developed[13]-[16]. Compressed sensing theory ensures that a sparse signal can be sampled in the case below Nyquist sampling rate, and completely reconstructed with the compressive samples. The development of compressed sensing makes the forms of compression be more extensive information expressions. In many applications, the final goal is detection or classification, which does not require the reconstruction of the compressed data. This allows implementing the detection and classification tasks directly from the compressed data, and is becoming a necessary and meaningful work.

The compressed expression can reduce the required amount of storage, but also brings about the difficulty for detection. The work in [17]-[18] made a try in this respect, and gave an example of direct use of compressed data for target detection and classification work. The work in [19] pointed out that the singular vectors obtained from the original data and the projected data have the same geometrical structure. Thus this paper proposes a method for defect detection and localization algorithm based on the projected

This work is supported by National Nature Science Foundation under Grant 61273170, 61304109, 61174142, 61034006.

*Corresponding Author

978-1-4799-3708-0/14/$31.00 

data without reconstruction. The main contributions are as follows:

1. We propose a method to detect and locate defects in the compressive framework, which is applicable to a wide variety of detection problems.

2. We employ the good characteristics of singular values of images, especially the stability and compressed invariance, to verify whether an image is defective. It is also suitable for compressive measurements.

3. We observe that the components of singular vectors of images reflect the relationship of their rows or columns, which is similar to latent semantic analysis. Based on the observation and the invariance of singular vectors, we locate the defect ranges of abnormal images.

## 2 Steel surface defect detection and localization for compressive data

### 2.1 Feasibility of flaw detection based on the singular value decomposition

Definition 2.1 Let $X = [x_1, x_2, \cdots, x_n] \in R^{m\times n}$ , without loss of generality, we assume $m \geq n$, the rank of the matrix $X$ is $r$, then there exist a unitary matrix $U = [u_1, u_2, \cdots, u_m] \in R^{m\times m}$, $V = [v_1, v_2, \cdots, v_n] \in R^{n\times n}$, such that

$$X = U\Sigma V^T = U \begin{bmatrix} \Sigma_r & 0 \\ 0 & 0 \end{bmatrix} V^T = U_r S_r V_r^T \quad (1)$$

where $S_r = diag[\sigma_1, \sigma_2, \cdots, \sigma_r]$, $\sigma_1 \geq \sigma_2 \geq \cdots \geq \sigma_r \geq 0$, $U_r \in R^{m\times r}$, $S_r \in R^{r\times r}$, $V_r^T \in R^{r\times n}$.
Formula (1) is called the singular value decomposition of the matrix $X$, and the column vectors $U$ and the column vectors $V$ are called left singular vectors and right singular vectors respectively, $\{\sigma_i, i = 1, \cdots, r\}$ are called the nonzero singular values of the matrix $X$. When $r < p = min\{m, n\}$, the matrix $X$ has $p - r$ zero singular values. $fv = \Sigma e = (\sigma_1, \sigma_2, \cdots, \sigma_r, 0, \cdots, 0)^T$ is the feature vector of the singular values of matrix $X$, wherein the column vector $e = (1, 1, \cdots, 1)^T \in R^{n\times 1}$.
The singular value decomposition is an important algebraic feature extraction method[20]-[23], one of its successful application is the latent semantic analysis[24]. The latent semantic analysis theory reveals that performing the singular value decomposition on the term-document matrix, one can find out the rough relationship among words or terms from the singular vectors. While an image is composed of rows or columns, the method similar to the latent semantic analysis can be used to determine the relationship among rows or columns, which indicates the defect information reflected by the singular vectors.
According to definition 2.1, an image can be approximated by a number of low-level sub-images based on the singular value decomposition, and the approximation error can be neglected. Since the approximation image is generated by the superposition of several sub-images, and each sub-image is spanned by the singular vectors and the singular values, so these singular vectors and singular values necessarily reflect the defect features when the image is defective. Thus it is feasible to verify the defection directly from the singular values and the singular vectors.
In addition, the singular values of an image has the properties of stability, scale invariance, transposition invariance, rotational invariance, shift invariance and mirror invariance[20]-[23]. Therefore, we use the singular values and the singular vectors for defect detection and localization.

### 2.2 Invariance of the data geometrical structure

#### 2.2.1 Invariance of the geometrical structure between columns of the raw data and its right singular vectors

Let the image matrix $X = [x_1, x_2, \cdots, x_n] \in R^{m\times n}$, perform the singular value decomposition on matrix $X$,

$$X = U\Sigma V^T = U_r S_r V_r^T = U_r Z_r \quad (2)$$

where $Z_r = S_r V_r^T = [z_1, z_2, \cdots, z_n]$, then $[x_1, x_2, \cdots, x_n] = U_r[z_1, z_2, \cdots, z_n]$, namely $x_i = U_r z_i$. Therefore we have

$$\|x_i\|_2^2 = x_i^T x_i = z_i^T U_r^T U_r z_i = \|z_i\|_2^2 \quad (3)$$

$$\|x_i - x_j\|_2^2 = \|U_r(z_i - z_j)\|_2^2 = \|z_i - z_j\|_2^2 \quad (4)$$

$$\frac{x_i^T x_j}{\|x_i\| \|x_j\|} = \frac{(U_r z_i)^T U_r z_j}{\|U_r z_i\| \|U_r z_j\|} = \frac{z_i^T z_j}{\|z_i\| \|z_j\|} \quad (5)$$

It is easily shown that the right singular vectors $\{z_i\}$ maintain the same geometrical structure of the columns $\{x_i\}$ of matrix $X$, $i = 1, \cdots, n$. It is also shown that the left singular vectors preserve the same geometrical structure among the rows $\{x_i\}$ of matrix $X$.

#### 2.2.2 Invariance of the geometrical structure between the right singular vectors of raw data and the right singular vectors of compressed data

In the framework of compressive sampling, the data was sampled before transmitting to the server. Let $x_i \in R^m$, we can get the compressed data $y_i = Px_i \in R^k$. Therefore, for the data matrix $X = [x_1, x_2, \cdots, x_n] \in R^{m\times n}$, we obtain

$$Y = [y_1, y_2, \cdots, y_n] = P[x_1, x_2, \cdots, x_n] = PX \quad (6)$$

where $Y \in R^{k\times n}$. After receiving the compressed data set $Y$, perform the singular value decomposition on the data $Y$, and obtain

$$Y = \hat{U}\hat{\Sigma}\hat{V}^T = \hat{U}_r \hat{S}_r \hat{V}_r^T = \hat{U}_r \hat{Z}_r \quad (7)$$

It is easily shown that the right singular vectors $\hat{Z}_r$ maintain the same geometrical structure of the columns of compressed data $Y$. According to formula(7), we can get a low-dimensional data set $\hat{Z}_r$ which is very close to $Z_r$ in the formula(2). Theorem 1[19] gives a guarantee that

the desired data set $\hat{Z}_r$ can be obtained. If $P \in R^{k\times m}$ is a random matrix satisfying the distributed Johnson-Lindenstrauss characteristic with

$$k \geq \frac{rlog(42/\epsilon) + log(2/\delta)}{f(\epsilon/\sqrt{2}))} \tag{8}$$

where $\epsilon \in (0,1)$ denotes a distortion factor, $\delta \in (0,1)$ denotes a failure probability, and $f(\cdot)$ is quadratic, then with probability exceeding $1-\delta$ for all $j = 1, 2, \cdots, r$, the following statements hold:

$$(1-\epsilon)^{1/2} \leq \frac{\hat{\sigma}_j}{\sigma_j} \leq (1+\epsilon)^{1/2} \tag{9}$$

where $\sigma_1 \geq \sigma_2 \geq ... \geq \sigma_r \geq 0$ denote the singular values of the raw data set $X$, and $\hat{\sigma}_1 \geq \hat{\sigma}_2 \geq \cdots \geq \hat{\sigma}_r \geq 0$ denote the singular value of the compressed data set $Y$.

$$\begin{aligned} &\|v_j - \hat{v}_j\|_2 \leq \\ &min\left\{\sqrt{2}, \frac{\epsilon\sqrt{1+\epsilon}}{\sqrt{1-\epsilon}} \max_{i\neq j} \frac{\sqrt{2}\sigma_i\sigma_j}{\min\limits_{c\in[-1,1]} |\sigma_i^2 - \sigma_j^2(1+c\epsilon)|}\right\} \end{aligned} \tag{10}$$

where $v_1, v_2, \cdots, v_r$ denote the right singular vectors of the raw data set $X$, and $\hat{v}_1, \hat{v}_2, \cdots, \hat{v}_r$ denote the right singular vectors of the compressed data set $Y$. The above statements guarantee that the preservation of the singular values and the right singular vectors for the raw data and the compressed data. Thus the right singular vectors $Z_r$ is very close to $\hat{Z}_r$, which is shown by the above theorem. In addition, the geometrical structure between the columns of raw data $X$ is preserved by its right singular vectors $Z_r$, which is shown by formula (3,4,5), it is also shown that the geometrical structure of the columns of compressed data $Y$ is maintained in its right singular vectors $\hat{Z}_r$. Therefore we can find out the geometrical structure between the columns of raw data is maintained in the columns of the compressed data. In other word, the compressive sampling process don't change the geometrical structure between the columns of raw data. We should note that Theorem 1[19] guarantees the preservation of the singular values and right singular vectors. Thus, we need another projection matrix $Q$ to sample $X$ in the right side. The similar conclusions can be obtained for the singular values and left singular vectors in a way the same as the proof of Theorem 1[19]. So the defect information in the raw data transferred into its singular vectors and singular values can also be obtained from the singular vectors and singular values of the compressed data. In the following section, we will use the singular vectors and singular values of the compressed data to verify the defects in the image without reconstructing operation. The steel strip surface defect detection algorithm based on compressed data consists of the defect detection algorithm based on singular values and the defect location algorithm based on singular vectors.

### 2.3 Defect detection algorithm based on the singular values of compressed data

#### 2.3.1 Compressive sampling of images

In the process of steel production, it is found that most of the steel products have excellent surface quality, so these images are normal images. Let the imaging conditions remain the same, in this case the pixel values of the normal images have only minor fluctuations. Compared with the defect images, the impact of such fluctuations on the singular values of the normal images is very small. It is shown that the singular values of the compressed image can remain unchanged. So here the singular values could be used to to determine whether an image is defective. Under compressed sensing framework, each image is compressively sampled. Take two image $X_1, X_2 \in R^{m\times n}$ for example, where $X_2$ is a normal image, let $P \in R^{k\times m}$ be a projection matrix, then $y_1 = PX_1, y_2 = PX_2$. Perform the singular value decomposition directly on the compressed data $y_1$ and $y_2$, and make use of the characteristics of singular values to determine whether the image $X_1$ is defective.

#### 2.3.2 Similarity measure of singular value feature vector

Let $fv$ denote the singular value vector of the compressed data $y_1$, and $\overline{fv}$ denote the singular value vector of the compressed data $y_2$, then

$$cos(\theta(fv, \overline{fv})) = \frac{\langle fv, \overline{fv}\rangle}{\|fv\|_2\|\overline{fv}\|_2} \tag{11}$$

If $\theta \leq T$, then the image $X_1$ is normal, otherwise the image $X_1$ is verified as a defective image, where $T$ is a threshold.

#### 2.3.3 Defect detection algorithm

The proposed defect detection algorithm based on singular values is described as follows:

- Step 1:Obtain the compressive data $y_1 = PX_1$, and let $y_2 = PX_2$ be the normal data sampled in advance, here $P$ is the projection matrix.
- Step 2:Perform the singular value decomposition on data $y_1$ and $y_2$, and obtain $fv$ and $\overline{fv}$ respectively.
- Step 3:Compute $\theta$ using $fv, \overline{fv}$. If $\theta \leq T$, then the image $X_1$ is a normal image, otherwise $X_1$ is verified as a defective image. Goto step 1.

### 2.4 Defect localization algorithm based on the singular vectors of compressed data

#### 2.4.1 selectivity of singular vectors

According to definition 2.1, an image can be approximated by a number of low-level sub-images spanned by the first few singular values, and the corresponding singular vectors, and the approximation error can be neglected. These singular vectors and singular values necessarily reflect the surface information of the original images. Then there is a question about the proper number of singular values and singular vectors to be picked out. The property of Frobenius norm of matrix shows that the energy is preserved in the sub-images after completing the singular value decomposition for an image. This means that the sum of squares of the singular values is equal to the sum of squares of all pixels in the image. In fact, the main energy is distributed

on the first few sub-images. It could be observed that the first 8 or even less singular values could occupy more than $90\%$ of the total energy, thus the first few sub-images corresponding to singular values can be used to approximate the desired image.

#### 2.4.2 Threshold criteria for defect localization

In terms of the cumulative contribution ratio of singular values, the first few singular vectors indicative of the range of possible defects is selected. If an image is defective, then the left singular vectors indicates the defect range in the vertical direction, while the right singular vectors indicates the defect range in the horizontal direction. In order to find defects in the image, take the right singular vectors $\hat{v}_i$ for example, define a symbol function $L(\cdot)$

$$L(j) = \begin{cases} 1, & abs(\hat{v}_i(j)) - mean(abs(\hat{v}_i)) \geq 0 \\ 0, & abs(\hat{v}_i(j)) - mean(abs(\hat{v}_i)) < 0 \end{cases} \quad (12)$$

where $abs(\cdot)$ is the absolute value function, $mean(\cdot)$ is the mean function, $i$ is the index of the right singular vector and $j$ is the index of the vector elements. If $L(j) = 1$, it indicates that the $jth$ column has defective pixels, otherwise it indicates that the $jth$ column has no defective pixels. we can verify that whether the $ith$ row has defective pixels in the same way after computing the symbol function for the left singular vector.

#### 2.4.3 Defect localization algorithm

The proposed defect localization algorithm based on singular vectors is described as follows:

- Step 1:Obtain the compressive data set $y_1 = PX_1$, and $\hat{y}_1 = X_1Q$, $P$ is the projection matrix.
- Step 2:Perform the singular value decomposition on data $y_1$ and $\hat{y}_1$, then obtain the right singular vector set $\hat{V}_r = [\hat{v}_1, \hat{v}_2, \cdots, \hat{v}_r]$ and the left singular vector set $\hat{U}_r = [\hat{u}_1, \hat{u}_2, \cdots, \hat{u}_r]$ respectively. Select the first few vectors corresponding the top singular values.
- Step 3:Compute the symbol function $L_{\hat{u}}$ for $\hat{u}_i$, and $L_{\hat{v}}$ for $\hat{v}_i$, and obtain the defect range $[indu_1^i, indu_2^i]$ in the vertical direction, and the defect range $[indv_1^i, indv_2^i]$ in the horizontal direction. Merge the defect ranges in the vertical direction into one range $[indu_1, indu_2]$, and merge the defect ranges in the horizontal direction into one range $[indv_1, indv_2]$ too. Then the area of the image defect can be determined as:

$$R = \begin{bmatrix} (indu_1, indv_1) & \cdots & (indu_1, indv_2) \\ \vdots & \ddots & \vdots \\ (indu_2, indv_1) & \cdots & (indu_2, indv_2) \end{bmatrix}$$

## 3 Experimental results

### 3.1 Defect detection experiment

Given a data set of 100 normal images, the disturbance of every image is Gaussian noise with 0 mean and variance 3. The random projection matrix $P, Q$ are used here to obtain compressed data. Then we get the compressive data set $y_i, i = 1, 2, \cdots, 100$, and perform the singular value decomposition on these compressed data. The result shows that the singular values satisfy stability, for example, randomly select 6 different compressive measurements, whose singular value vectors are shown in Table 1, each containing the top 16 singular values . Consider another 100 images including two types of defects: rectangular convex defect, rectangular concave defects, each category accounts for 40 percent of the total images, 20 percent of them are normal images. Use the above projection matrix $P$ to compress the images, and obtain the compressed data $y_i, i = 1, 2, \cdots, 100$. Select randomly 6 different compressed data from these measurements, and perform the singular value decomposition on them, whose singular value vectors are shown in Table 2, each containing the top 16 singular values. The first two singular value vectors indicate the corresponding images are normal, which is in accordance with Table 1, and the last four singular value vectors indicate the corresponding image are defective, where the symbol "$\surd$" indicates normal, and the symbol "$\times$" indicates abnormal. Table 2 shows the top 16 singular values of differences of images to be test and the normal image. Figure 1 shows the detection result, the abscissa denotes the index of the images to be tested. If the tested image is abnormal, the vertical axis is the value of its index, otherwise the value is set to zero.

Table 1: The singular values of normal images

| fv | 1($\surd$) | 2($\surd$) | 3($\surd$) | 4($\surd$) | 5($\surd$) | 6($\surd$) |
|---|---|---|---|---|---|---|
| 1st | 26054 | 26061 | 26049 | 26049 | 26052 | 26051 |
| 2nd | 85.8 | 83.8 | 84.3 | 86.2 | 82.7 | 83.4 |
| 3rd | 82.3 | 81.6 | 80.0 | 82.5 | 80.2 | 81.6 |
| 4th | 77.9 | 80.8 | 79.2 | 80.9 | 78.0 | 80.3 |
| 5th | 77.1 | 79.8 | 76.4 | 77.9 | 76.6 | 77.5 |
| 6th | 76.2 | 76.3 | 74.9 | 76.9 | 74.1 | 76.3 |
| 7th | 75.2 | 75.1 | 73.5 | 75.6 | 73.2 | 73.2 |
| 8th | 72.5 | 74.4 | 72.1 | 73.2 | 72.1 | 71.8 |
| 9th | 71.5 | 71.7 | 70.2 | 72.0 | 70.1 | 70.7 |
| 10th | 70.1 | 70.8 | 69.1 | 71.8 | 68.4 | 69.4 |
| 11th | 69.2 | 69.8 | 68.8 | 70.3 | 66.9 | 68.2 |
| 12th | 68.3 | 68.2 | 68.1 | 68.3 | 66.2 | 64.8 |
| 13th | 68.0 | 66.3 | 66.2 | 66.3 | 65.2 | 64.3 |
| 14th | 66.3 | 65.6 | 65.6 | 65.7 | 64.4 | 63.3 |
| 15th | 65.6 | 64.5 | 63.6 | 65.1 | 63.3 | 62.9 |
| 16th | 64.1 | 63.3 | 62.8 | 63.5 | 62.7 | 61.4 |

### 3.2 Defect localization experiment

The second set of images are used to test the localization algorithm. According to the result of previous section, if the tested image is defective, then perform the localization algorithm on the corresponding compressive measurements. The obtained defect regions are shown in Table 3. Figure 2 shows the defective information in the original images, where images (1,1)-(1,4) is normal images, and images (2,1)-(2,4) are corresponding to the result of the first four rows of Table 3, images (3,1)-(3,4) are corresponding to the result of the $5th - 8th$ rows of Table 3, image (4,1)-(4,4) are corresponding to the result of the $9th - 12th$ rows

Table 2: The singular values of differences of images to be test and the normal image

| fv | 1($\surd$) | 2($\surd$) | 3($\times$) | 4($\times$) | 5($\times$) | 6($\times$) |
|---|---|---|---|---|---|---|
| 1st | 26053 | 26054 | 28486 | 27539 | 25028 | 25281 |
| 2nd | 84.0 | 84.8 | 3503 | 3205 | 3433 | 3063 |
| 3rd | 81.1 | 80.6 | 281.0 | 261.7 | 237.6 | 216.0 |
| 4th | 80.6 | 78.7 | 270.9 | 248.5 | 228.5 | 212.2 |
| 5th | 77.1 | 77.2 | 263.5 | 232.6 | 220.8 | 189.0 |
| 6th | 76.4 | 76.8 | 253.2 | 225.9 | 213.2 | 184.2 |
| 7th | 75.4 | 74.9 | 247.6 | 219.8 | 203.4 | 178.8 |
| 8th | 74.0 | 73.4 | 242.2 | 209.8 | 195.3 | 168.9 |
| 9th | 73.4 | 71.0 | 232.5 | 202.1 | 191.3 | 164.3 |
| 10th | 69.4 | 69.7 | 230.4 | 187.5 | 184.7 | 162.5 |
| 11th | 69.1 | 69.0 | 221.3 | 180.5 | 175.6 | 156.3 |
| 12th | 67.3 | 67.8 | 214.5 | 177.3 | 169.6 | 143.0 |
| 13th | 66.8 | 66.9 | 213.4 | 172.5 | 167.0 | 140.3 |
| 14th | 64.8 | 65.4 | 204.9 | 169.6 | 161.3 | 136.4 |
| 15th | 64.0 | 64.6 | 198.5 | 166.7 | 156.7 | 132.7 |
| 16th | 63.4 | 63.2 | 195.8 | 163.7 | 153.3 | 129.6 |

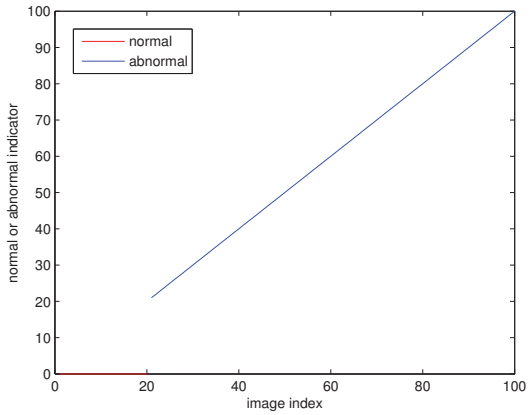


Figure 1: The detection result for normal and abnormal images.

of Table 3, images (5,1)-(5,4) are corresponding to the result of the last four rows of Table 3.

## 4 Conclusion

This paper proposed a method for defect detection and localization algorithm based on the singular value decomposition and compressive data. The singular value decomposition is used to maintain the energy contained in the original image, further it is shown that the energy and pattern can be transferred from the original image into the singular values and singular vectors of compressive data. Thus we give a defect detection algorithm without reconstruction. In the future work, we will consider the classification task based on compressive sampling.

## REFERENCES


[1] Roland T. Chin, Charles A. Harlow, Automated visual inspection: a survey, IEEE Transactions on Pattern Analysis and Machine Intelligence, 4(6), 557-573, 1982.

[2] Timothy S. Newman, Anil K. Jain, A survey of automated visual inspection, Computer vision and image understanding, 61(2), 1995.


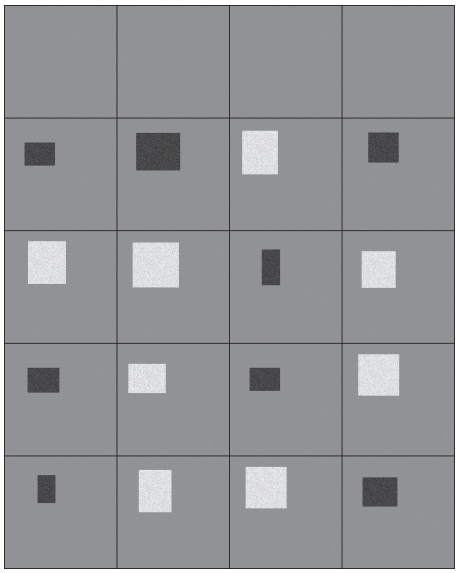

Figure 2: The original images containing normal and abnormal ones.

Table 3: Defect region

| defect range | $indu_1$ | $indu_2$ | $indv_1$ | $indv_2$ |
|---|---|---|---|---|
| (2,1) | 56 | 108 | 46 | 115 |
| (2,2) | 34 | 119 | 44 | 144 |
| (2,3) | 29 | 128 | 29 | 110 |
| (2,4) | 33 | 101 | 60 | 129 |
| (3,1) | 24 | 121 | 54 | 140 |
| (3,2) | 27 | 129 | 36 | 141 |
| (3,3) | 43 | 124 | 74 | 115 |
| (3,4) | 47 | 130 | 45 | 122 |
| (4,1) | 56 | 112 | 53 | 125 |
| (4,2) | 47 | 113 | 26 | 111 |
| (4,3) | 56 | 108 | 46 | 115 |
| (4,4) | 25 | 119 | 37 | 130 |
| (5,1) | 44 | 107 | 76 | 116 |
| (5,2) | 32 | 128 | 50 | 124 |
| (5,3) | 25 | 119 | 37 | 130 |
| (5,4) | 49 | 115 | 47 | 126 |


[3] T. Ojala, M. Pietikainen and T. Maenpaa, Multiresolution Gray-Scale and Rotation Invariant Texture Classification with Local Binary Patterns, IEEE Transactions on Pattern Analysis and Machine Intelligence, 24(7), 2002.

[4] Hong-Dar Lin, Computer-aided visual inspection of surface defects in ceramic capacitor chips, Journal of Materials Processing Technology, 189(1-3), 2007.

[5] Kenneth R. Castleman, Digital image processing. Prentice Hall, 2007

[6] Xianghua Xie, Majid Mirmehdi, TEXEMS: Texture Exemplars for Defect Detection on Random Textured Surfaces, IEEE transactions on Pattern analysis and machine intelligence, 2007

[7] Anders Landstrom, matthew J.Thurley, morphology-based crack detection for steel slabs, IEEE journal of selected topics in signal processing, 2012.

[8] Mohammadreza Yazdchi, Mehran Yazdi, Arash Golibagh

Mahyari, Steel Surface Defect Detection Using Texture Segmentation Based on Multifractal Dimension, International Conference on Digital Image Processing, 2009.
[9] Mostafa Sadeghi, Masoud Shafiee, Mohsen Shafieirad, A new approach to improve defect detection of steel sheets using gabor wavelet. International Journal of Information and Electronics Engineering,2013
[10] Luiz A.O. Martins, Flávio L.C. P*á*dua, Paulo E.M. Almeida, Automatic detection of surface defects on rolled steel using Computer Vision and Artificial Neural Networks, 36th Annual Conference on IEEE Industrial Electronics Society, 2010
[11] Jonathan Masci, Ueli Meier, Dan Ciresan,Jürgen Schmidhuber, Gabriel Fricout, Steel defect classification with Max-Pooling Convolutional Neural Networks. the 2012 International Joint Conference on Neural Networks, 2012
[12] Wu-bin Li,Chang-houLu n, Jian-chuanZhang, A lower envelope Weber contrast detection algorithm for steel bar surface pit defects. Optics and Laser Technology, 2013
[13] Emmanuel Candes, Justin Romberg, Terence Tao. Robust uncertainty principles: Exact signal reconstruction from highly incomplete frequency information, IEEE Transactions on Information Theory, 52(2), 489-509, 2006
[14] Emmanuel Candes, Terence Tao, Near-optimal signal recovery from random projections: Universal encoding strategies?, IEEE Transactions on Information Theory, 52(12), 5406-5425, 2006,
[15] David Donoho, Compressed sensing, IEEE Transactions on Information Theory, 52(4), 1289-1306, 2006
[16] Emmanuel Candes, M.B. Wakin, An introduction to compressive sampling. IEEE Signal Processing Magazine, 25(2): 21-30, 2008
[17] M.A. Davenport, P.T. Boufounos, M.B. Wakin, R. G. Baraniuk, signal processing with compressive measurements, IEEE Journal of Selected Topics in Signal Processing, vol.4,no.2, pp.445-460,2010.
[18] James E. Fowler, Qian Du, Anomaly detection and reconstruction from random projections. IEEE transactions on image processing, vol.21,no.1,2012
[19] Anna C. Gilbert, Jae Young Park, Michael B. Wakin, Sketched SVD:recovering spectral features from compressive measurements. arXiv preprint arXiv:1211.0361, 2012.
[20] Lloyd N.Trefethen and David.Bau,III.Numerical linear algebra, Society for Industrial and Applied Machematics, Philadelphia, 1997.
[21] Carl D. Meyer, Matrix analysis and applied linear algebra, Society for Industrial and Applied Machematics, Philadelphia, 2000.
[22] V.C. Klema, A.J. Laub, The singular value decomposition: its computation and some applications.IEEE Transactions on Automatic Control,AC-25(2),1980.
[23] Ziquan Hong, Algebraic Feature extraction of image for recognition, Pattern Recognition, 24(3),1991.
[24] Christopher D. Manning, Prabhakar Raghavan, Hinrich Schtze, Introduction to Information Retrieval. Cambridge University Press, 2008